Figure 1

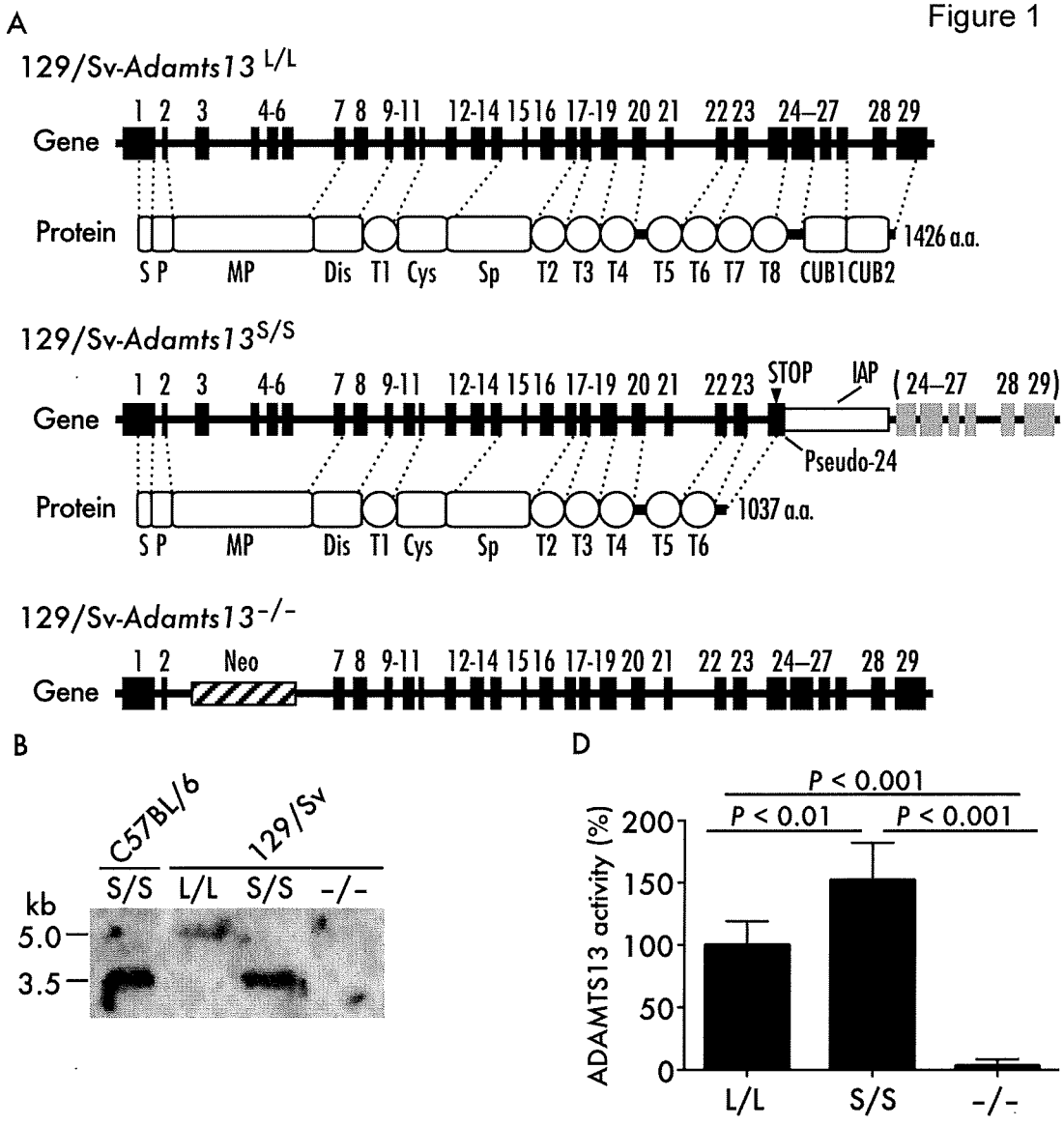
A
129/Sv-Adamts13 L/L
Gene
1 2 3 4-6 7 8 9-11 12-14 15 16 17-19 20 21 22 23 24–27 28 29
Protein
1426 a.a.
S P MP Dis T1 Cys Sp T2 T3 T4 T5 T6 T7 T8 CUB1 CUB2
129/Sv-Adamts13 S/S
STOP
IAP
( 24–27 28 29)
Pseudo-24
1037 a.a.
S P MP Dis T1 Cys Sp T2 T3 T4 T5 T6
129/Sv-Adamts13 -/-
Neo
B
C57BL/6
129/Sv
S/S L/L S/S -/-
kb
5.0
3.5
D
P < 0.001
P < 0.01
P < 0.001
ADAMTS13 activity (%)
200
150
100
50
0
L/L S/S -/-
C
Pooled L/L (%)
0 50 100 200 400
L/L
1 2 3
S/S
1 2 3
-/-
1 2 3
Substrate
Product
Pooled L/L (%)
0 50 100 200 400
L/L
4 5 6
S/S
4 5 6
-/-
4 5 6
Substrate
Product

Figure 2

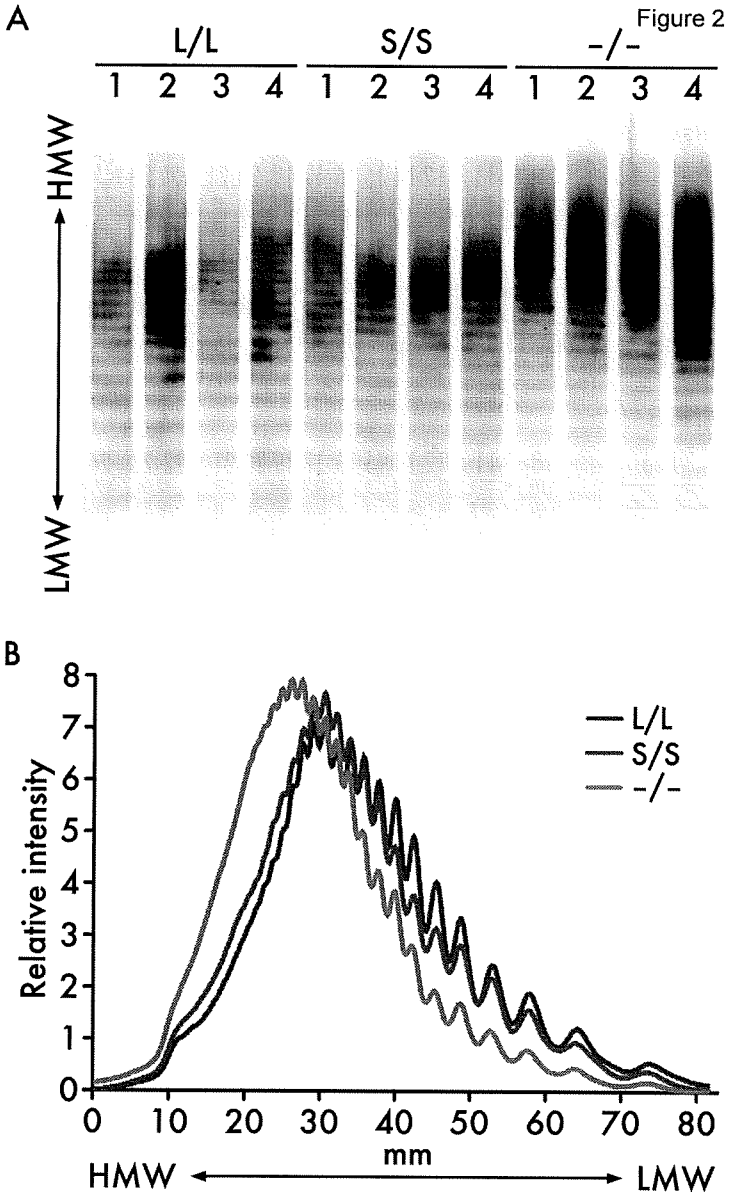
A
L/L
S/S
-/-
1 2 3 4 1 2 3 4 1 2 3 4
HMW
LMW
B
Relative intensity
0 1 2 3 4 5 6 7 8
0 10 20 30 40 50 60 70 80
mm
HMW
LMW
L/L
S/S
-/-

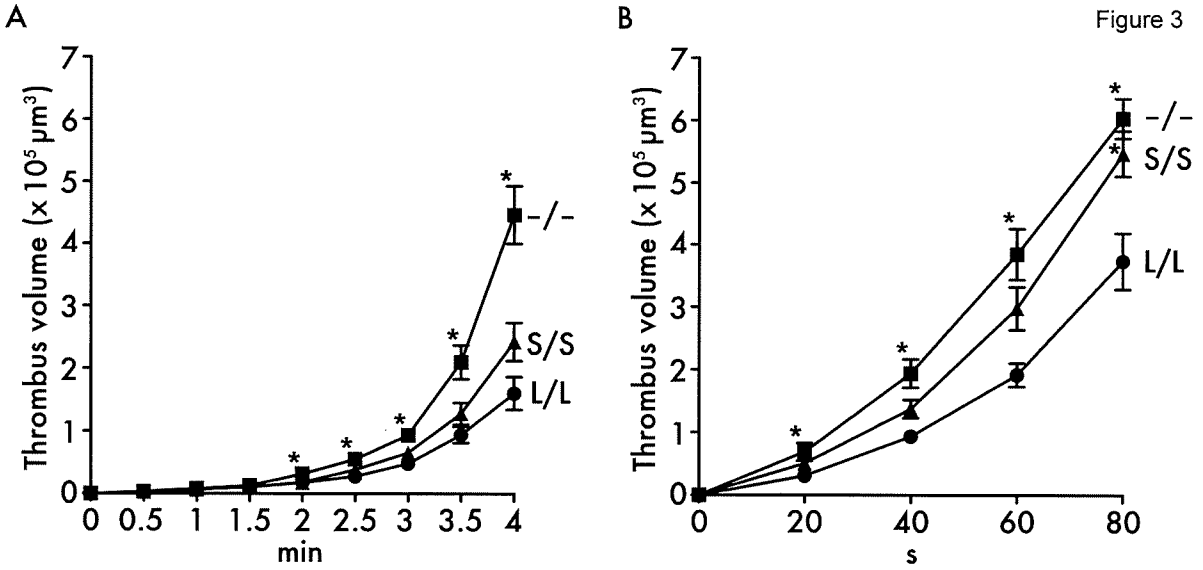
A
B
Thrombus volume (x 10⁵ µm³)
min
s
-/-
S/S
L/L
0
0.5
1
1.5
2
2.5
3
3.5
4
20
40
60
80
*

Figure 3

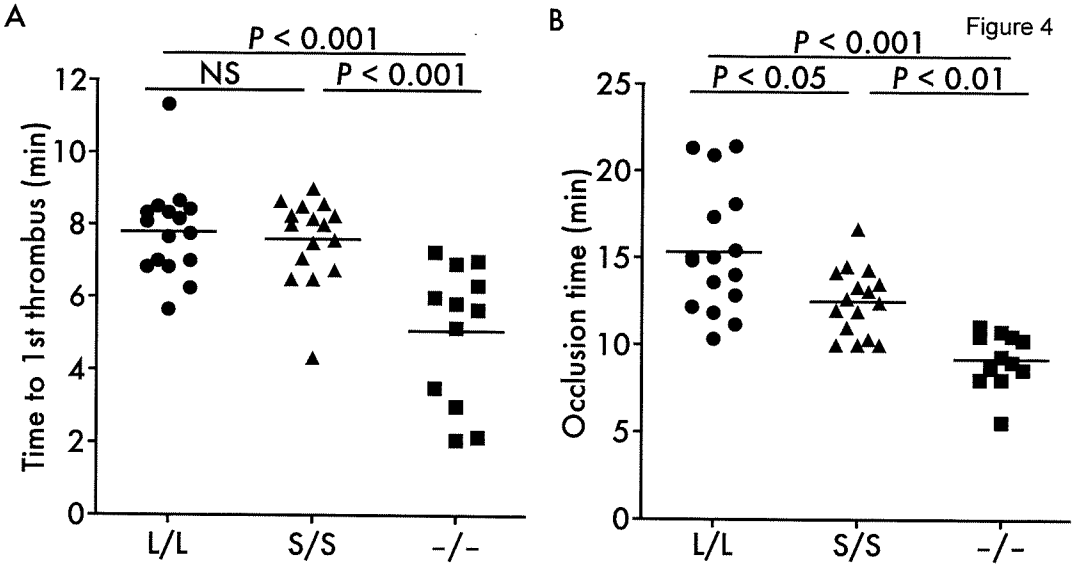
A
P < 0.001
NS
P < 0.001
Time to 1st thrombus (min)
12
10
8
6
4
2
0
L/L
S/S
-/-
B
P < 0.001
P < 0.05
P < 0.01
Occlusion time (min)
25
20
15
10
5
0
L/L
S/S
-/-

Figure 4

Figure 5

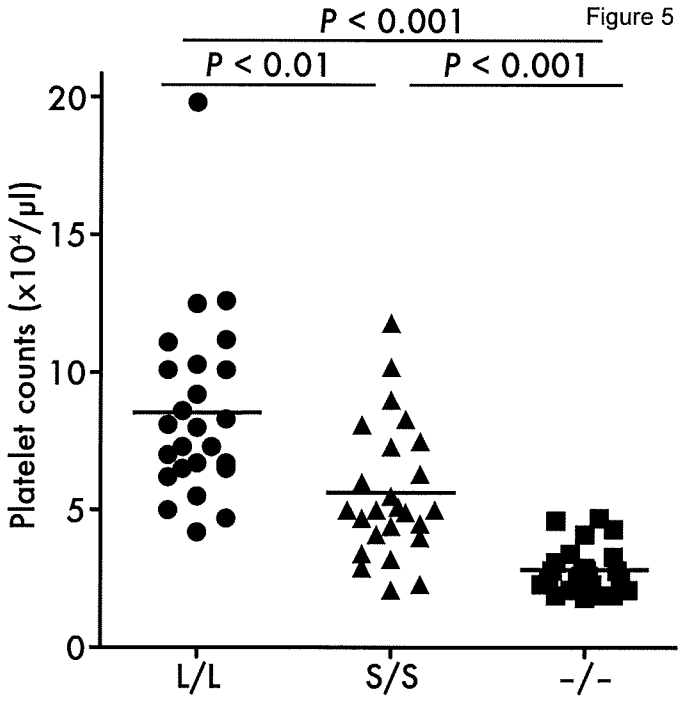

ELSEVIER

Brain & Development 31 (2009) 717–724

BRAIN & DEVELOPMENT
Official Journal of the Japanese Society of Child Neurology

www.elsevier.com/locate/braindev

Original article

# Intracerebral cell transplantation therapy for murine GM1 gangliosidosis

Tomo Sawada [a], Akemi Tanaka [a,*], Katsumi Higaki [c], Ayumi Takamura [c], Eiji Nanba [c], Toshiyuki Seto [a,e], Mitsuyo Maeda [b], Etsuko Yamaguchi [a], Junichiro Matsuda [d], Tunekazu Yamano [a]

[a] *Department of Pediatrics, Osaka City University Graduate School of Medicine, 1-4-3 Asahi-machi, Abeno-ku, Osaka 545-8585, Japan*
[b] *Department of Neurobiology and Anatomy, Osaka City University Graduate School of Medicine, Osaka, Japan*
[c] *Division of Functional Genomics, Research Center for Bioscience and Technology, Tottori University, Yonago, Japan*
[d] *Laboratory of Experimental Animal Models, Division of Bioresources, National Institute of Biomedical Innovation, Osaka, Japan*
[e] *Department of Pediatrics, Fujiidera City Hospital, Fujiidera, Japan*

Received 25 August 2008; received in revised form 15 October 2008; accepted 1 November 2008

**Abstract**

We performed a cell transplantation study to treat the brain involvement in lysosomal storage diseases. We used acid β-galactosidase knock-out mice (BKO) from C57BL/6 as recipients. To minimize immune responses, we used cells derived from transgenic mice of C57BL/6 overexpressing the normal human β-galactosidase. Fetal brain cells (FBC), bone marrow-derived mesenchymal stem cells (MSC), and mixed FBC and MSC cells were prepared and injected into the ventricle of newborn BKO mouse brain. The mice were examined at 1, 2, 4, and 8 weeks and 6 months after injection. In each experiment, the injected cells migrated into the whole brain effectively and survived for at least 8 weeks. Decrease in ganglioside GM1 level was also observed. FBC could survive for 6 months in recipient brain. However, the number of transplanted FBC decreased. In the brains of MSC- or mixed cell-treated mice, no grafted cells could be found at 6 months. To achieve sufficient long-term effects on the brain, a method of steering the immune response away from cytotoxic responses or of inducing tolerance to the products of therapeutic genes must be developed.


*Keywords:* GM1-gangliosidosis; Cell transplantation; Fetal brain cell; Mesenchymal stem cell

## 1. Introduction

Enzyme replacement therapy (ERT), hematopoeitic stem cell transplantation (HSCT), and gene transfer have been studied in animals and in humans with lysosomal storage disease (LSD). ERT is now available clinically for Gaucher disease, Fabry disease, Pompe disease, and MPS I, II, and VI in many countries, and has been successful in visceral organs. HSCT is also effective against the somatic involvements in Gaucher disease and MPS I, II, and VI. However, HSCT exhibits little efficacy in conditions such as Fabry disease and Pompe disease, when enzyme secretion from donor cells is poor or the uptake of enzyme proteins by the affected host cells is inadequate. In addition, efficacy in individual organs differs markedly, in both ERT and HSCT, depending on accessibility of blood flow and the density of mannose-6-phosphate receptors. Neither HSCT nor ERT exhibits efficacy against the brain involvement in Gaucher or MPSs because of the poor access due to the blood–brain barrier.

Many experimental studies have been carried out, involving methods such as gene therapy [1–5], cell

* Corresponding author. Tel.: +81 6 6645 3816; fax: +81 6 6636 8737.
*E-mail address:* akemi-chan@med.osaka-cu.ac.jp (A. Tanaka).

0387-7604/$ - see front matter © 2008 Elsevier B.V. All rights reserved.
doi:10.1016/j.braindev.2008.11.004

therapy [6–9], or intrathecal administration of enzymes [10,11], for treatment of the brain in LSDs. Such treatments were able to overcome the blood–brain barrier to access brain tissue and exhibit considerable efficacy in brain. However, it is difficult to maintain such efficacy for long periods of time. Repetition of these treatments is not practical because intracranial administration is required for them. On the other hand, the usefulness of intravenous administration is limited because of the blood–brain barrier, except in newborn mice which have an immature barrier. It has been reported that intravenous administration of extremely high doses of enzymes [12–14] or of enzymes that remain in the circulation for long periods [15,16] yielded slight passage through the blood–brain barrier, though with increase in the risk of immune response.

Oral administration of small molecules would be a good and convenient method of treatment of the brain for prolonged periods, such as substrate reduction therapy with *N*-butyldeoxynojirimycin or *N*-butyldeoxygalactonojirimycin for glycosphingolipidoses [17–19] or genistein for mucopolysaccharidoses [20], and chemical chaperone therapy for Fabry disease [21] or GM1-gangliosidosis [22]. However, the efficacy of substrate reduction therapies has thus far been quite limited, and chemical chaperone therapies are not applicable for every type of gene mutation.

GM1 gangliosidosis is an LSD and a progressive neurological disease in humans caused by a genetic defect of lysosomal acid β-galactosidase, which hydrolyses the terminal β-galactosidic residue of ganglioside GM1 and other glycoconjugates. The defects in β-galactosidase activity result in accumulation of ganglioside GM1 in various organs, especially the brain, causing progressive neurodegeneration. In our previous study [2], we injected recombinant adenovirus encoding mouse β-galactosidase cDNA intravenously in β-galactosidase-deficient newborn mice, and showed that vector-mediated β-galactosidase-producing brain cells could reduce ganglioside GM1 accumulation. We showed that β-galactosidase enzyme protein could be secreted as well as taken up by the brain cells and function effectively. However, the efficacy obtained was transient. If sufficient amounts of the defective enzyme could be permanently secreted by cells in the brain, injury of the brain could be prevented. To examine the possibility of long-term cell treatment of the brain in LSDs, we carried out a transplantation experiment in the brain of a GM1-gangliosidosis mouse model (acid β-galactosidase knock-out mouse) using fetal brain cells (FBC) and mesenchymal stem cells (MSC) from bone marrow. These cells used for transplantation were derived from mice of the same genetic background as recipient mice except for possession of the human β-galactosidase gene.

## 2. Materials and methods

### 2.1. Knock-out and transgenic mice

A mouse model of GM1 gangliosidosis (BKO mouse) was generated by targeting of the β-galactosidase gene at exon 15 in ES cells as previously described [23]. Newborn mice were obtained by mating heterozygous female mice with homozygous male mice. Identification of newborn mutants was accomplished by quantitative analysis of β-galactosidase activity in tail tip homogenates on the day of birth. Mice with high β-galactosidase activity (TG mice) [24] were generated by introducing the human β-galactosidase gene as a transgene in ES cells obtained from the BKO mouse, which has several copies of the human β-galactosidase gene without the mouse β-galactosidase background. Age-matched wild-type mice of C57BL/6 strain were used as a control.

### 2.2. Cell preparations for transplantation

Cultured mesenchymal stem cells (MSC) were obtained from the bone marrow of the tibias and femurs of 5–8 month-old TG mice according to the method of Meirelles et al. [25] with some modifications. Dulbecco's modified Eagle's medium (DMEM: Sigma Chemical Co., St Louis, MO) containing 10% fetal bovine serum (Medical and Biological Laboratories, Nagoya, Japan) was used for culture.

Fetal brain cells (FBC) were obtained from the fetal cerebral cortex of TG mice at 13 days of gestation according to the method of Meberg and Miller [26]. The brain tissue was disrupted in a Pasteur glass pipette by gentle stroking several times (uncultured FBC), and then cultured for 4 h in Neurobasal medium (Invitrogen, Carlsbad, CA, No. 12348-07) containing 2 mM glutamine and 10% FBS, followed by two days in Neurobasal medium containing 2 mM glutamine and B27 supplement (Invitrogen, No. 14175-095) (cultured FBC).

### 2.3. Transplantation of cells into newborn mouse brain

Each BKO mouse received a single injection of 0.5–1.0 $\times 10^5$ of the cells prepared as described above in the right cerebral ventricle from 24 to 48 hours after birth. Study groups were as follows: uncultured FBC ($n = 18$), cultured FBC ($n = 10$), MSC ($n = 17$), and mixed MSC and FBC (1:1) ($n = 15$). Mice of each experimental group were divided into three subgroups for X-gal staining, β-galactosidase assay and ganglioside GM1 analysis. Mice were examined at one, two, four, and eight weeks and 6 months after injection as shown in Table 1.

For biochemical analysis, mice were anesthetized with diethylether and the blood was washed out with normal saline by perfusion through the heart, and the

brains were removed and kept at −80 °C until use. For histological studies, the brains were fixed by perfusion through the heart with 4% paraformaldehyde in 0.1 M phosphate buffer pH 7.4 (PB) for 20 min., after washing out the blood with normal saline. To obtain frozen sections, the brains were placed in 0.1 M phosphate buffer pH 7.4 containing 30% sucrose, and frozen in liquid nitrogen.

All surgical and care procedures were carried out in accordance with the Guidelines for Use and Care of Experimental Animals approved by the Animal Committee of Osaka City University School of Medicine.

### 2.4. X-Gal staining

Frozen sections (16 μm thick) were reacted with X-gal using the β-gal staining Kit (Invitrogen Corp., Carlsbad, CA) to visualize β-galactosidase activity.

### 2.5. β-Galactosidase assay

β-Galactosidase activity was analyzed in the tissue homogenate with the artificial substrate 2 mM 4-methylumbelliferyl β-galactoside at pH 4.0 in 0.1 M sodium citrate-phosphate buffer according to the method described by Suzuki [27]. Protein was analyzed using the Bio-Rad protein assay system (Bio-Rad Laboratories, Hercules, CA) with the method of Bradford [28].

### 2.6. Analysis of ganglioside GM1

Amounts of ganglioside GM1 were measured by immunoblot assay using anti-GM1 ganglioside monoclonal antibody (Code: 370685, Seikagaku Corp., Tokyo, Japan) by the method of Michikawa et al. [29] with some modifications.

Brain tissue cells were disrupted by sonication and solubilized in 20 mM Tris–HCl buffer pH 8.0 containing 137 mM NaCl, 10% glycerol, and a protease inhibitor cocktail (Complete, Mini, Cat No. 11836153001, Roche Diagnostics, Mannheim, Germany). Five micrograms of tissue protein was applied onto Trans-Blot Transfer Medium Pure Nitrocellulose Membrane (0.45 μm pore size, Code: 162-0117, Bio-Rad Laboratories) through the slots of a Bio-Dot SF Microfiltration Apparatus (Bio-Rad Laboratories). The membrane was reacted with anti-GM1 ganglioside monoclonal antibody diluted 1:500, after blocking with 5% skim milk in PBS solution for 1 h at room temperature, and then with horseradish peroxidase-linked anti-mouse IgG sheep antibody (Code: NA931, GE Healthcare UK Ltd., Buckinghamshire, UK) diluted 1:1,000. The washing solution used was 0.1 M Tris buffered saline pH 7.5 containing 0.1% Tween 20 (TTBS). Bound antibody was detected using ECL after reaction with ECL™ Western Blotting Detection Reagents (Code: RPN2209, GE Healthcare UK Ltd.) and visualized on X-ray film. Densitometric quantification of immunoreactive signal was performed using the Kodak Digital Science™ EDAS 120 system with 1D Image Analysis software (Eastman Kodak Company, NY). The values obtained were compared with those of quantification of histological immunoreactivity with Leica Control Software as previously described [30], and the same ratios were obtained among the samples (data not shown). The assay was performed three times and in duplicate for each sample independently, and mean values were calculated.

## 3. Results

### 3.1. X-Gal staining

Layered staining of the transplanted cells was observed over the entire ventricular surface on both sides of the cerebral hemispheres in treated mice at one week after injection (data not shown). Positive cells had spread into the brain tissue by two weeks (Fig. 1c and f) in the mice treated with cultured FBC ($n = 1$), uncultured FBC ($n = 1$), and MSC ($n = 2$) in the same amounts. The cells had spread further and had reached every part of the brain by 4 weeks in the mice of all experimental groups (Fig. 1d, g and i). Less positive cells were found in the mice treated with MSC ($n = 3$) or mixed MSC and FBC ($n = 3$) (Fig. 1g and i) than in the mice treated with cultured ($n = 3$) or uncultured FBC ($n = 3$) (Fig. 1d). The number of the X-Gal positive cells increased gradually until 4 weeks after injection in every experimental mouse. At 8 weeks after injection, positive cells still existed in the cultured FBC- ($n = 3$) and uncultured FBC-treated ($n = 3$) mice (Fig. 1e) in the same numbers with a similar distribution as at 4 weeks. However, a significant decrease in number of positive cells was found at 8 weeks in the mice treated with MSC ($n = 3$) or mixed MSC and FBC ($n = 3$) (Fig. 1h and j). In the mice treated with mixed MSC and FBC, positive cells existed in higher numbers in deep areas than in the mice treated with MSC alone. In the mice treated with cultured ($n = 2$) and uncultured FBC ($n = 2$), small numbers of positive cells with strong staining still existed in many parts of the brain, especially around the striatum and lateral globs pallidus (Fig. 1k and l), at 6 months after injection. No grafted cells were found in the mice treated with MSC ($n = 1$) or mixed MSC and FBC ($n = 1$) at 6 months. No significant differences were noted among the mice within each experimental group at each stage.

### 3.2. β-Galactosidase activity

The β-galactosidase activity in FBC and MSC derived from TG mice were 214.5–227.5 nmol/mg/h ($n = 4$) and 143.0–121.4 nmol/mg/h ($n = 3$), respec-

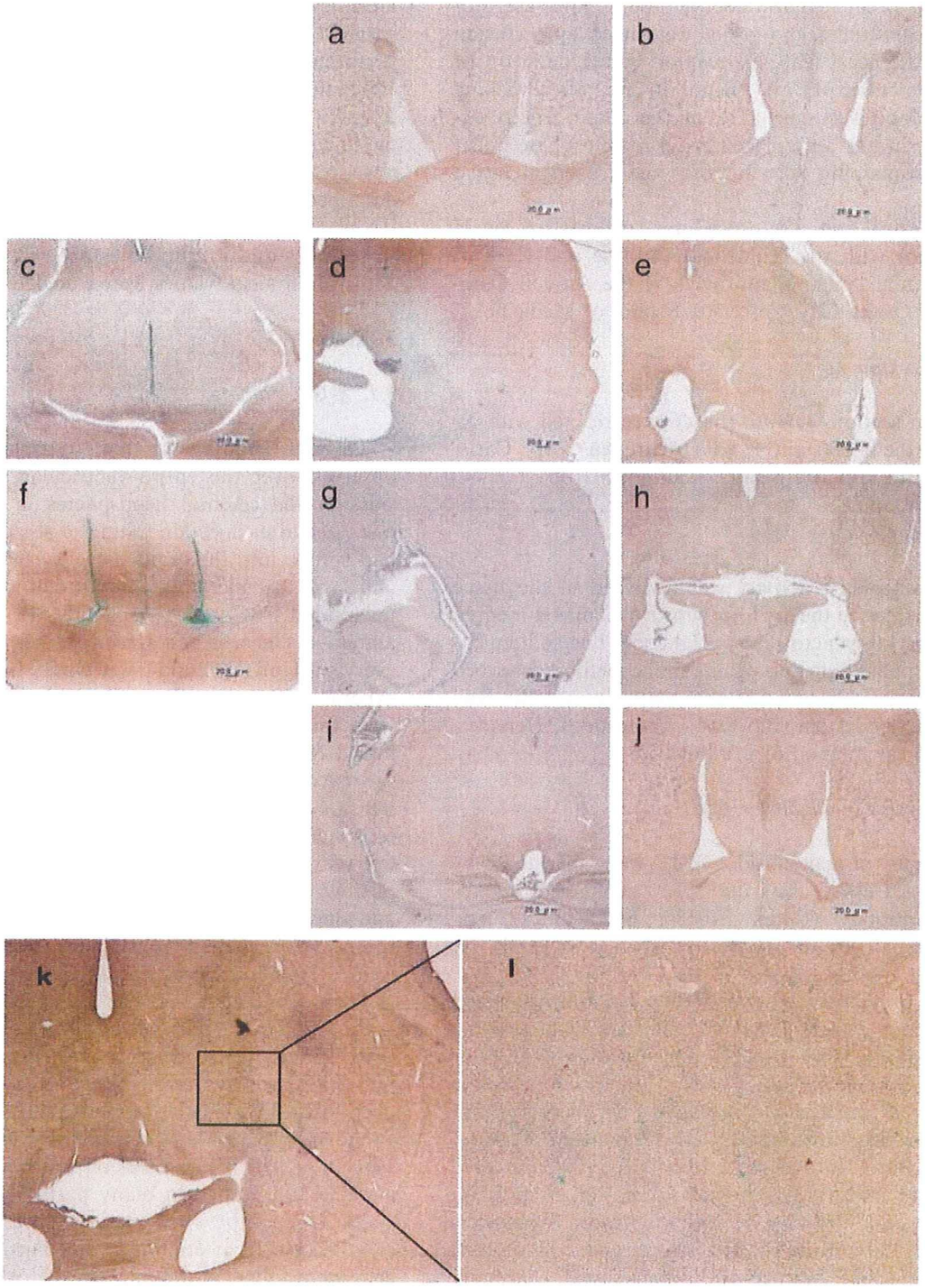


Fig. 1. X-Gal staining of brain coronal sections at +0.8 mm to −2.0 mm of bregma. (a and b) Non-treated BKO mouse at 4 and 8 weeks old, respectively; (c–e) Treated with FBC at 2, 4, and 8 weeks after injection; (f–h) Treated with MSC at 2, 4, and 8 weeks after injection; (i and j) Treated with mixed MSC and FBC at 4 and 8 weeks after injection; (k) FBC-treated brain at 6 months after injection; (l) Magnification of figure k. Positive cells had spread into the brain tissue by two weeks (c and f). The cells had spread further by 4 weeks (d, g and i). Less positive cells were found in the mice treated with MSC or mixed MSC and FBC (g and i) than in the mice treated with FBC (d). At 8 weeks, positive cells still existed in FBC-treated mouse (e) as at 4 weeks (d). A significant decrease in number of positive cells was found at 8 weeks in the mice treated with MSC (h) or mixed MSC and FBC (j). Strong positive staining cells still existed at 6 months in the brain of FBC-treated mouse (k and l).

tively, while the activity in FBC and in MSC derived from wild-type mice were 54.9–69.1 ($n = 2$) and 63.0 ($n = 1$), respectively.

The results of brain β-galactosidase activity in transplantation experiments are shown in Table 2. Increases in β-galactosidase activity were found in the brains of each experimental group at 4 weeks after injection. Activity in the FBC-treated mice was definitely increased at 4 weeks as well as at 8 weeks, while activity at 8 weeks in the MSC-treated mice and mixed MSC and FBC-treated mice was almost the same level as that in the untreated mice. These findings were consistent with those in the X-Gal staining study.

### 3.3. Immunoassay of ganglioside GM1

Immunoassay of accumulated ganglioside GM1 was performed for each mouse using anti-GM1 ganglioside monoclonal antibody. Values are ratios to the amounts in age-matched normal control mice. The results are shown in Fig. 2 and Tables 3. At 4 weeks after injection, remarkable decrease in ganglioside GM1 accumulation

Table 1
Mouse numbers used for each experiment.

| Time after injection | 1 week | 2 weeks | 4 weeks | 8 weeks | 6 months |
|---|---|---|---|---|---|
| | [X-Gal staining] | | | | |
| Uncultured FBC | 1 | 1 | 3 | 3 | 2 |
| Cultured FBC | 1 | 1 | 3 | 3 | 2 |
| MSC | | 2 | 3 | 3 | 1 |
| Mixed MSC and FBC | | | 3 | 3 | 1 |
| | [β-galactosidase activity] | | | | |
| Uncultured FBC | | | 2 | 2 | |
| Cultured FBC | | | | | |
| MSC | | | 2 | 2 | |
| Mixed MSC and FBC | | | 2 | 2 | |
| | [Immunoblot assay of ganglioside GM1 amount] | | | | |
| Uncultured FBC | | | 1 | 1 | 1 |
| Cultured FBC | | | | | |
| MSC | | | 2 | 2 | |
| Mixed MSC and FBC | | | 2 | 2 | |

Table 2
β-Galactosidase activity.

| | 4 weeks | 8 weeks |
|---|---|---|
| Age-matched normal control (mean ± SD) | 197 ± 61 ($n = 7$) | 159 ± 56 ($n = 7$) |
| Non-treated (mean ± SD) | 4.38 ± 0.35 ($n = 5$) | 4.10 ± 0.47 ($n = 5$) |
| Treated with uncultured FBC | Mouse 1 | Mouse 7 |
| | Rt: 6.65[a] | Rt: 4.94 |
| | Lt: 5.31[a] | Lt: 6.03[a] |
| | Mouse 2 | Mouse 8 |
| | Rt: 7.36[a] | Rt: 5.58[a] |
| | Lt: 5.33[a] | Lt: 5.05[a] |
| Treated with MSC | Mouse 3 | Mouse 9 |
| | Rt: 6.30[a] | Rt: 4.13 |
| | Lt: 5.95[a] | Lt: 3.67 |
| | Mouse 4 | Mouse 10 |
| | Rt: 5.74[a] | Rt: 4.19 |
| | Lt: 5.12[a] | Lt: 5.05[a] |
| Treated with mixed MSC and FBC | Mouse 5 | Mouse 11 |
| | Rt: 5.80[a] | 4.13 (mix of both hemispheres) |
| | Lt: 5.40[a] | |
| | Mouse 6 | Mouse 12 |
| | Rt: 5.06 | Rt: 4.85 |
| | Lt: 4.52 | Lt: 5.02 |

Values are in nmol/mg/h. Each sample was tested in duplicate and results are mean values. Rt, right hemisphere; Lt, left hemisphere.
[a] Increase of activity over mean + 2SD of non-treated mice.

Table 3
Immunoblot assay of ganglioside GM1 amount.

| | 4 weeks | 8 weeks | 6 months |
|---|---|---|---|
| Age-matched non-treated (range) | 2.65–3.55 ($n = 3$) | 4.98–5.28 ($n = 3$) | 7.58 (n = 1) |
| Treated with uncultured FBC | Mouse I | Mouse VI | Mouse XI |
| | Rt: 1.42[a] | Rt: 2.30[a] | Rt: 6.18[b] |
| | Lt: 1.80[a] | Lt: 2.44[a] | Lt: 6.40[b] |
| Treated with MSC | Mouse II | Mouse VII | |
| | Rt: 1.82[a] | Rt: 5.30 | |
| | Lt: 1.31[a] | Lt: 5.23 | |
| | Mouse III | Mouse VIII | |
| | Rt: 1.40[a] | Rt: 4.40[b] | |
| | Lt: 1.34[a] | Lt: 4.73[b] | |
| Treated with mixed MSC and FBC | Mouse IV | Mouse IX | |
| | Rt: 1.33[a] | Rt: 4.55[b] | |
| | Lt: 1.34[a] | Lt: 4.78[b] | |
| | Mouse V | Mouse X | |
| | Rt: 1.78[a] | Rt: 4.45[b] | |
| | Lt: 1.62[a] | Lt: 4.58[b] | |

Values are ratios to those for age-matched control mice. Each sample was tested in duplicate for three times and results are mean values. Rt, right hemisphere; Lt, left hemisphere.
[a] Remarkable decrease.
[b] Slight decrease of ganglioside GM1 compared with non-treated mice.

was found in the mice of every group. However, at 8 weeks, decrease was detected only in the mouse treated with FBC. Efficacy was still noted at 6 months after injection in FBC-treated mouse. These findings were consistent with those for X-Gal staining (Fig. 1) and β-galactosidase activity (Table 2).

## 4. Discussion

Two therapeutic methods, HSCT and ERT, are clinically available for LSDs. However, neither is markedly effective in the brain. A number of experiments in animal models have been carried out on the treatment of brain in LSDs. Each revealed some efficacy in the brain, though it was transient and incomplete. Sufficient enzyme expression throughout life is needed in the brain. Thus, permanent engraftment of enzyme-secreting cells in the brain, or permanent expression of an exogenous gene with a vector or as an integrated gene might eliminate the brain involvement in LSDs.

However, the immune responses of host animals are among the most difficult problems to overcome in this respect [31–33]. Although the brain, which is sequestered from systemic immune responses, is thought to exhibit little immune response, elimination of cells expressing a therapeutic transgene occurs in the brain. We speculate that innate inflammatory immune responses are stimulated to kill such cells, not necessarily with the induction of a linked adaptive immune response. When host brain cells express a therapeutic transgene mediated by a viral vector, the host cells themselves will be eliminated, possibly resulting in acceleration of neuronal cell death in neurodegenerative disorders. Transplantation of cells having the same genetic information as the host animals with LSD except for expression of a deficient enzyme protein would thus be a good method of treatment for avoiding the elimination of host neuronal cells and curing diseased host cells.

We performed cell transplantation into the brain of β-galactosidase-deficient mice to study the usefulness of long-term engraftment for supplementation of deficient enzyme protein. To minimize the immune responses in the recipient β-galactosidase knock-out mice, we used cells of mice with the same genetic background as the recipient except for possession of copies of the human β-galactosidase gene.

Initially, in the transplantation experiment, we used FBC from transgenic mice expressing the human β-galactosidase gene. The cells could grow in an environment similar to that of the recipient organ in which they were originally growing. The cells spread into the brains and the cell number increased at least until 4 weeks. They grew very successfully for at least 8 weeks and survived for 6 months or more. However, the number of engrafted cells had decreased significantly at 6 months, while the size of the brain had increased. The decrease in ganglioside GM1 accumulation was also marked until 8 weeks after transplantation. However, at 6 months, this decrease was far less pronounced, with re-accumulation of ganglioside GM1. After the cells were engrafted and the cell number was increased by the cell division in the recipient brain, they were depleted. The mechanism of depletion of transplanted cells involved immunological rejection, although the transplanted cells were very similar genetically and physiologically to the recipient.

Next, we performed a transplantation experiment using MSCs obtained from the bone marrow of the

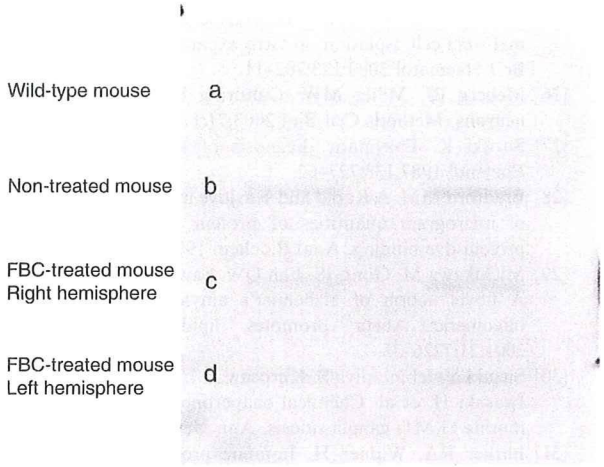


Fig. 2. Immunoblot assay of ganglioside GM1 in brain homogenate at 8 weeks after treatment. Performed in duplicate as shown in two slots for each sample. (a) Wild-type mouse; (b) Non-treated mouse; (c and d) Right and left hemisphere, respectively, of a mouse treated with FBC. The immunoreactivity against ganglioside GM1 antibody in the treated brain (c and d) was less than non-treated brain (d). The accumulated amounts of ganglioside GM1 were calculated in the ratio to the age-matched wild-type mouse (a) from the densitometric quantification signals. These values were shown in Table 3.

same mice expressing the human β-galactosidase gene. MSCs were obtained using the method of plastic adherence. This relatively crude procedure produces a heterogeneous population including multipotential MSCs. These crude cells were used to avoid depletion of potentially important cells and for ease of preparation for clinical application. The cells spread into the brains and the cell number increased similarly to FBC transplantation experiment until 4 weeks. However, decrease in number of engrafted living cells and efficacy in preventing accumulation of ganglioside GM1 were observed in the examination of 8-week-old treated mice.

A number of studies on neural transdifferentiation have been reported [34–37]. Some have reported that neural transdifferentiation of MSCs is induced by cell fusion with host neuronal cells [38–41]. We therefore used mixed FBC and MSC cells to stimulate cell fusion. More engrafted cells were found in the deep areas of the mouse brains treated with mixed cells than in the brains treated with MSC alone. However, no fused cells could be identified. The long-living cells were probably transplanted FBC themselves.

Decrease of ganglioside GM1 was observed even though the increase of the β-galactosidase activity was so small. Similar efficacy was shown previously in our gene therapy experiment [2]. On the other hand, we observed a general depletion of the transplanted cells over time in the BKO mouse brains. The transplanted cells survived in early stage and the number increased by cell division, then, died. This was likely caused by immunological rejection, even though we used fetal brain cells (FBC) from mice with the same genetic background for transplantation. We speculated that immunological reaction occurred because these cells expressed the therapeutic enzyme protein which the host animals did not have. The same has been reported in the transplantation of autogenous cells expressing an exogenous therapeutic gene [33]. The grafted cells were gradually depleted because of immunological rejection by the host animals. To avoid deleterious immune attack and to achieve sufficient long-term efficacy in brain, development of methods to steer the immune response away from cytotoxic responses or to induce tolerance to the products of therapeutic genes is needed [42,43].

## Acknowledgements

We thank Kaoru Takano and Takanori Kunieda for mating of mice and providing the BKO and TG mice in timely fashion for each experiment.

This work was supported by grant AT-18591163 from the Ministry of Education, Culture, Sports, Science, and Technology of Japan.

## References

[1] Shen JS, Watabe K, Ohashi T, Eto Y. Intraventricular administration of recombinant adenovirus to neonatal twitcher mouse leads to clinicopathological improvements. Gene Ther 2001;8:1081–7.

[2] Takaura N, Yagi T, Maeda M, Nanba E, Oshima A, Suzuki Y, et al. Attenuation of ganglioside GM1 accumulation in the brain of GM1 gangliosidosis mice by neonatal intravenous gene transfer. Gene Ther 2003;10:1487–93.

[3] Kim EY, Hong YB, Lai Z, Cho YH, Brady RO, Jung SC. Long-term expression of the human glucocerebrosidase gene in vivo after transplantation of bone-marrow-derived cells transformed with a lentivirus vector. J Gene Med 2005;7:878–87.

[4] Shen JS, Meng XL, Yokoo T, Sakurai K, Watabe K, Ohashi T, et al. Widespread and highly persistent gene transfer to the CNS by retrovirus vector in utero: implication for gene therapy to Krabbe disease. J Gene Med 2005;7:540–51.

[5] Cachón-González MB, Wang SZ, Lynch A, Ziegler R, Cheng SH, Cox TM. Effective gene therapy in an authentic model of Tay-Sachs-related diseases. Proc Natl Acad Sci USA 2006;103:10373–8.

[6] Kopen GC, Prockop DJ, Phinney DG. Marrow stromal cells migrate throughout forebrain and cerebellum, and they differentiate into astrocytes after injection into neonatal mouse brains. Proc Natl Acad Sci USA 1999;96:10711–6.

[7] Jin HK, Carter JE, Huntley GW, Schuchman EH. Intracerebral transplantation of mesenchymal stem cells into acid sphingomyelinase-deficient mice delays the onset of neurological abnormalities and extends their life span. J Clin Invest 2002;109:1183–91.

[8] Sakurai K, Iizuka S, Shen JS, Meng XL, Mori T, Umezawa A, et al. Brain transplantation of genetically modified bone marrow stromal cells corrects CNS pathology and cognitive function in MPS VII mice. Gene Ther 2004;11:1475–81.

[9] Givogri MI, Galbiati F, Fasano S, Amadio S, Perani L, Superchi D, et al. Oligodendroglial progenitor cell therapy limits central

neurological deficits in mice with metachromatic leukodystrophy. J Neurosci 2006;26:3109–19.
[10] Kakkis E, McEntee M, Vogler C, Le S, Levy B, Belichenko P, et al. Intrathecal enzyme replacement therapy reduces lysosomal storage in the brain and meninges of the canine model of MPS I. Mol Genet Metab 2004;83:163–74.
[11] Dickson P, McEntee M, Vogler C, Le S, Levy B, Peinovich M, et al. Intrathecal enzyme replacement therapy: successful treatment of brain disease via the cerebrospinal fluid. Mol Genet Metab 2007;91:61–8.
[12] Vogler C, Levy B, Grubb JH, Galvin N, Tan Y, Kakkis E, et al. Overcoming the blood–brain barrier with high-dose enzyme replacement therapy in murine mucopolysaccharidosis VII. Proc Natl Acad Sci USA 2005;102:14777–82.
[13] Matzner U, Herbst E, Hedayati KK, Lüllmann-Rauch R, Wessig C, Schröder S, et al. Enzyme replacement improves nervous system pathology and function in a mouse model for metachromatic leukodystrophy. Hum Mol Genet 2005;14:1139–52.
[14] Blanz J, Stroobants S, Lüllmann-Rauch R, Morelle W, Lüdemann M, D'Hooge R, et al. Reversal of peripheral and central neural storage and ataxia after recombinant enzyme replacement therapy in {alpha}-mannosidosis mice. Hum Mol Genet 2008;17:3437–45.
[15] Grubb JH, Vogler C, Levy B, Galvin N, Tan Y, Sly WS. Chemically modified {beta}-glucuronidase crosses blood–brain barrier and clears neuronal storage in murine mucopolysaccharidosis VII. Proc Natl Acad Sci USA 2008;105:2616–21.
[16] Montaño AM, Oikawa H, Tomatsu S, Nishioka T, Vogler C, Gutierrez MA, et al. Acidic amino acid tag enhances response to enzyme replacement in mucopolysaccharidosis type VII mice. Mol Genet Metab 2008;94:178–89.
[17] Kasperzyk JL, El-Abbadi MM, Hauser EC, D'Azzo A, Platt FM, Seyfried TN. *N*-butyldeoxygalactonojirimycin reduces neonatal brain ganglioside content in a mouse model of GM1 gangliosidosis. J Neurochem 2004;89:645–53.
[18] Lachmann RH, te Vruchte D, Lloyd-Evans E, Reinkensmeier G, Sillence DJ, Fernandez-Guillen L, et al. Treatment with miglustat reverses the lipid-trafficking defect in Niemann-Pick disease type C. Neurobiol Dis 2004;16:654–8.
[19] Cox TM. Substrate reduction therapy for lysosomal storage diseases. Acta Paediatr Suppl. 2005;94:69–75.
[20] Piotrowska E, Jakóbkiewicz-Banecka J, Barańska S, Tylki-Szymańska A, Czartoryska B, Wegrzyn A, et al. Genistein-mediated inhibition of glycosaminoglycan synthesis as a basis for gene expression-targeted isoflavone therapy for mucopolysaccharidoses. Eur J Hum Genet 2006;14:846–52.
[21] Ishii S, Yoshioka H, Mannen K, Kulkarni AB, Fan JQ. Transgenic mouse expressing human mutant alpha-galactosidase A in an endogenous enzyme deficient background: a biochemical animal model for studying active-site specific chaperone therapy for Fabry disease. Biochim Biophys Acta 2004;1690:250–7.
[22] Matsuda J, Suzuki O, Oshima A, Yamamoto Y, Noguchi A, Takimoto K, et al. Chemical chaperone therapy for brain pathology in G(M1)-gangliosidosis. Proc Natl Acad Sci USA 2003;100:15912–7.
[23] Matsuda J, Suzuki O, Oshima A, Ogura A, Noguchi Y, Yamamoto Y, et al. Beta-galactosidase-deficient mouse as an animal model for GM1-gangliosidosis. Glycoconj J 1997;14:729–36.
[24] Yamamoto Y, Nagase Y, Noguchi A, Mochida K, Nakahira M, Takano K, et al. Generation and characterization of the β-galactosidase knockout mouse having the normal human β-galactosidase gene as a transgene (in Japanese). Proc Jap Soc of Animal Models for Hum Dis (Nippon Shikkan Model Gakkai Kiroku) 2001;17:20–2.
[25] Meirelles Lda S, Nardi NB. Murine marrow-derived mesenchymal stem cell: isolation, in vitro expansion, and characterization. Br J Haematol 2003;123:702–11.
[26] Meberg PJ, Miller MW. Culturing hippocampal and cortical neurons. Methods Cell Biol 2003;71:111–27.
[27] Suzuki K. Enzymatic diagnosis of sphingolipidosis. Methods Enzymol 1987;138:727–62.
[28] Bradford MM. A Rapid and sensitive method for the quantitation of microgram quantities of protein utilizing the principle of protein-dye binding. Anal Biochem 1976;72:255–60.
[29] Michikawa M, Gong JS, Fan QW, Sawamura N, Yanagisawa K. A novel action of alzheimer's amyloid beta-protein (Abeta): oligomeric Abeta promotes lipid release. J Neurosci 2001;21:7226–35.
[30] Suzuki Y, Ichinomiya S, Kurosawa M, Ohkubo M, Watanabe H, Iwasaki H, et al. Chemical chaperone therapy: clinical effect in murine G(M1)-gangliosidosis. Ann Neurol 2007;62:671–5.
[31] Barker RA, Widner H. Immune problems in central nervous system cell therapy. NeuroRx 2004;1:472–81.
[32] Abordo-Adesida E, Follenzi A, Barcia C, Sciascia S, Castro MG, Naldini L, et al. Stability of lentiviral vector-mediated transgene expression in the brain in the presence of systemic antivector immune responses. Hum Gene Ther 2005;16:741–51.
[33] Lowenstein PR, Kroeger K, Castro MG. Immunology of neurological gene therapy: how T cells modulate viral vector-mediated therapeutic transgene expression through immunological synapses. Neurotherapeutics 2007;4:715–24.
[34] Weimann JM, Charlton CA, Brazelton TR, Hackman RC, Blau HM. Contribution of transplanted bone marrow cells to Purkinje neurons in human adult brains. Proc Natl Acad Sci USA 2003;100:2088–93.
[35] Abouelfetouh A, Kondoh T, Ehara K, Kohmura E. Morphological differentiation of bone marrow stromal cells into neuron-like cells after co-culture with hippocampal slice. Brain Res 2004;1029:114–9.
[36] Wislet-Gendebien S, Hans G, Leprince P, Rigo JM, Moonen G, Rogister B. Plasticity of cultured mesenchymal stem cells: switch from nestin-positive to excitable neuron-like phenotype. Stem cells 2005;23:392–402.
[37] Deng J, Petersen BE, Steindler DA, Jorgensen ML, Laywell ED. Mesenchymal stem cells spontaneously express neural proteins in culture and are neurogenic after transplantation. Stem cells 2006;24:105410–64.
[38] Terada N, Hamazaki T, Oka M, Hoki M, Mastalerz DM, Nakano Y, et al. Bone marrow cells adopt the phenotype of other cells by spontaneous cell fusion. Nature 2002;416:542–5.
[39] Alvarez-Dolado M, Pardal R, Garcia-Verdugo JM, Fike JR, Lee HO, Pfeffer K, et al. Fusion of bone-marrow-derived cells with Purkinje neurons, cardiomyocytes and hepatocytes. Nature 2003;425:968–73.
[40] Kozorovitskiy Y, Gould E. Stem cell fusion in the brain. Nat Cell Biol 2003;5:952–4.
[41] Bae JS, Furuya S, Shinoda Y, Endo S, Schuchman EH, Hirabayashi Y, et al. Neurodegeneration augments the ability of bone marrow-derived mesenchymal stem cells to fuse with Purkinje neurons in Niemann-Pick type C mice. Hum Gene Ther 2005;16:1006–11.
[42] Tomatsu S, Gutierrez M, Nishioka T, Yamada M, Yamada M, Tosaka Y, et al. Development of MPS IVA mouse (Galnstm(hC79S. mC76S)slu) tolerant to human *N*-acetylgalactosamine-6-sulfate sulfatase. Hum Mol Genet 2005;14:3321–5.
[43] Matzner U, Matthes F, Herbst E, Lüllmann-Rauch R, Callaerts-Vegh Z, D'Hooge R, et al. Induction of tolerance to human arylsulfatase A in a mouse model of metachromatic leukodystrophy. Mol Med 2007;13:471–9.

*Exp. Anim. 57(4), 385–395, 2008*

# *Type 2 Diabetes Mellitus in a Non-Obese Mouse Model Induced by* Meg1/Grb10 *Overexpression*

Yoshie YAMAMOTO[1, 2)], Fumitoshi ISHINO[3)], Tomoko KANEKO-ISHINO[4)], Hirosuke SHIURA[3)], Kozue UCHIO-YAMADA[5)], Junichiro MATSUDA[5)], Osamu SUZUKI[5)], and Katsunori SATO[2)]

*[1)]Department of Veterinary Science, National Institute of Infectious Diseases, 1–23–1 Toyama, Shinjuku-ku, Tokyo 162-8640, [2)]Okayama University Graduate School of Natural Science and Technology, 3–1–1 Tsushima-naka, Okayamashi, Okayama 700-8530, [3)]Department of Epigenetics, Medical Research Institute, Tokyo Medical and Dental University, 1–5–45 Yushima, Bunkyou-ku, Tokyo 113-8510, [4)]Tokai University School of Health Sciences, Bohseidai, Isehara, Kanagawa 259-1193, and [5)]Division of Biomedical Research Resources, National Institute of Biomedical Innovation, 7–6–8 Saito-Asagi, Ibaraki, Osaka 567-0085, Japan*

***Abstract:*** *We assessed the possibility of C57BL/6-Tg (*Meg1/Grb10*)isn(Meg1 Tg) mice as a non-obese type 2 diabetes (2DM) animal model. Meg1 Tg mice were born normal, but their weight did not increase as much as normal after weaning and showed about 85% of normal size at 20 weeks of age. Body mass index of Meg1 Tg mice was also smaller than that of control mice. The glucose tolerance test and insulin tolerance test showed that Meg1 Tg mice had reduced ability to normalize the blood glucose level. Blood urea nitrogen (BUN) in Meg1 Tg mice (19.6 ± 1.2 mg/dl) was significantly lower than in controls (22.0 ± 0.8 mg/dl), while plasma triglyceride, insulin, adiponectin, and resistin levels were significantly higher (202.0 ± 23.4 mg/dl vs 146.3 ± 23.4 mg/dl, 152.4 ± 16.3 pg/ml vs 88.1 ± 16.9 pg/ml, 74.4 ± 10.9 μg/ml vs 48.3 ± 7.0 μg/ml, and 4.0 ± 0.2 ng/ml vs 3.6 ± 0.2 ng/ml, respectively). Body, visceral fat weight and liver weights were significantly lower (19.6 ± 0.4 g vs 24.3 ± 0.3 g, 376.7 ± 29.6 mg to 507.5 ± 23.0 mg, and 906.0 ± 41.8 mg to 1,001.0 ± 15.1 mg, respectively). Thus, hyperinsulinemia observed in Meg1 Tg mice indicates that their insulin signaling pathway is somehow inhibited. With high fat diet, the diabetes onset rate of Meg1 Tg mice increased up to 60%. These results suggest that Meg1 Tg mice resemble human 2DM.*

***Key words:*** *biochemical characterization,* Meg1/Grb10 *transgenic mouse, non-obese mouse model, type 2 diabetes mellitus*

## Introduction

Type 2 diabetes mellitus (2DM) is a life-threatening endocrine disorder that affects as many as 6% to 10% of the population of the world. This type of diabetes is classified as non-insulin dependent diabetes and accounts for higher than 95% of all cases of diabetes [12, 39]. Moreover, recent studies have revealed that the prevalence of 2DM has doubled in the United States over the last 30 years [1].

*(Received 2 November 2007 / Accepted 24 March 2008)*

*Address corresponding: Y. Yamamoto, Department of Veterinary Science, National Institute of Infectious Diseases, 1–23–1 Toyama, Shinjuku-ku, Tokyo 162-8640, Japan*

Many experimental 2DM model animals have been established from spontaneous mutants and are currently in use in human 2DM research [11, 22, 24, 33, 35]. In spite of much effort, which has focused on using such model animals, some aspects of 2DM remain unclear. To elucidate the pathological character of 2DM, it is necessary to identify which metabolic pathways are responsible for the onset of 2DM. However, in many cases, the relationship between original mutations and their affected metabolic pathways is difficult to explain. Recent progress in molecular biology has enabled us to take another approach to develop novel diabetes model animals through the manipulation of genes that are closely related to glucose metabolism and insulin resistance [6]. Using gene-targeting technology, a number of useful mouse models have recently been developed for the study of the progression of diabetes [4, 17].

Recently, genomic imprinting has been discovered as an important factor in the etiology of 2DM. A number of studies have reported a relationship between genomic imprinting and 2DM in the mouse [13, 21, 30]. Overexpression of some imprinted genes might explain the mechanism of human transient neonatal diabetes [21], and deletion of some imprinted genes has been suggested as the cause of pancreatic $\beta$ cell dysfunction [13]. Another candidate imprinted gene for 2DM is maternally expressed 1(Meg1)/ growth factor receptor-binding protein (Grb) 10 [23]. Recently, it has been reported that *Meg1/Grb10* knockout mice show the embryonic overgrowth phenotype [3]. *Meg/Grb10* transgenic mice Meg1 Tg mice were produced to elucidate Meg1/Grb10 function *in vivo* [31]. Grb10 interacts with both insulin receptors (IR) and insulin-like growth factor I receptors (IGF-1R) *in vitro* [8, 9, 27]. Since the IGF-1 signaling pathway is reportedly involved in embryonic growth, Meg1/Grb10 may have a negative effect both on the embryonic growth and postnatal growth phenotypes associated with uniparental duplication of chromosome 11 [7, 23]. Alternatively, Meg1/Grb10 may function in glucose homeostasis, which is regulated by the IR signaling pathway. Insulin binds to IR and activates a signal transduction pathway through its receptor kinase activity. It has been demonstrated that IGF1 functions via IGF1R, while IGF2 functions via both IGF1R and IR, and that each of these signaling pathways contributes to some extent to late embryonic growth [20]. Moreover, mutation studies of human 2DM patients indicate the existence of additional factors in the pathogenesis of this disease [25].

Overall, Meg1 Tg mice have similar character to human 2DM in overexpression of the imprinted Meg1/Grb10 gene that functions negatively for both insulin signaling via IR and IGF-1 signaling via IGF-1R. Therefore, it seems likely that, in the late embryonic stage, when endogenous Meg1/Grb10 expression is very high, Meg1/Grb10 negatively regulates growth via modulation of both the IR and IGF1R cascades [31]. There are few data about biochemical changes in the Meg1 Tg mouse. To be useful in therapeutic research the model mouse has to show a similar phenotype to human 2DM. Furthermore, the incidence rate of the onset of 2DM in Meg1 Tg mice fed on basal diet was reportedly small [30].

In this study, we examined several basic biochemical characters of Meg1 Tg mice as a 2DM model, and the effects of diet on the onset of 2DM. The results indicate that the Meg1 Tg mouse is a useful non-obese 2DM mouse model.

## Materials and Methods

*Animals*

The production and maintenance of *Meg1/Grb10* transgenic mice were reported in detail at elsewhere [31]. Transgenic (C57BL X C3H) $F_2$ mice were screened by PCR amplification of tail DNA samples using transgene-specific and endogenous Peg1 primer sets. Transgenic-positive founder mice (Meg1 Tg mouse) were backcrossed to C57BL/6NJcl (C57BL/6) mice, and the litters that were used in subsequent studies contained animals that were maintained within the C57BL/6 hybrid background. The Meg1 Tg mouse consists of 4 lines, with names of T10L, T18L, T20L, and T27L. We used these 4 lines for each experiment. Transgenic-negative mice were used as control mice. C57BL/6, NOD/ShiJcl (NOD), KK-$A^y$/TaJcl (KK-$A^y$), and BKS.Cg-+$Lepr^{db}$/+$Lepr^{db}$/Jcl (BKS) mice were also used in the RT-PCR experiment. Only male mice were used in our experiment.

This study was performed in accordance with the *Guidelines for Animal Experimentation of the National*

*Institute of Infectious Diseases.*

*Body weight and body mass index (BMI)*

Body weights of all mice used in our experiments were measured weekly from 4 weeks of age to 20 weeks. At 15 weeks of age, mouse length from nose to anus was recorded. Body mass index (BMI) was calculated as body weight (g) / body length$^2$ (cm).

*Food and water intake*

The mice were allowed free access to food pellets and water. We used either CMF (Oriental yeast Co., Ltd., Tokyo) or Quick Fat (CLEA Japan, Inc., Tokyo) for normal fat diet (NFD) and high fat diet (HFD), respectively. HFD contains high crude fat and glucose, which gives it a higher calorie count than NFD. Food intake per mouse was calculated as the average of 3 days intake at 11 weeks of age.

*Organ weight*

At 30 weeks of age 5 Meg1 Tg mice and control mice were sacrificed under deep ether anesthesia and necropsied. Visceral fat and livers were separated and weighed.

*Glucose tolerance test and insulin tolerance test*

Glucose tolerance tests and insulin tolerance test were performed on 11-week-old Meg1 Tg mice that had been fed on HFD. Glucose tolerance tests and insulin tolerance tests were performed after overnight fasting by administering glucose orally (2.0 g/kg body weight) and 0.3 $\mu$l of blood was collected from the tail vain after 0, 30, 60, and 120 min. The blood glucose level was measured by FreeStyle Meter (NIPRO, Osaka). Insulin tolerance tests were performed by an intraperitoneal injection of 1.0 U/kg of human insulin (Eli Lilly Japan, Tokyo) to Meg1 Tg mice and control mice; then 0.3 $\mu$l of blood was collected from the tail vein after 0, 30, 60, and 90 min. The blood glucose level was measured by FreeStyle Meter (NIPRO).

*Plasma chemistry*

Meg1 Tg and control mice were maintained on a normal light/dark cycle. Blood was collected from the mice with heparin at necropsy and inspection. The samples were centrifuged at 13,000 rpm centrifugation, and plasma was collected and stored at –30°C until assay. Plasma leptin, adiponectin, insulin and resistin were assayed by ELISA. Plasma total glucose, total cholesterol (TCHO), ammonia, triglyceride (TG), blood urea nitrogen (BUN), GOT, GPT, ALP, CPK, and LDH were measured using Fuji dry-chem 3000 (FUJIFILM Medical Co., Ltd., Tokyo). Livers and visceral adipose tissues were also recorded.

*Histology*

For histopathology, pancreas tissue samples were taken from Meg1 Tg and control mice at 20 weeks of age. The tissue samples were fixed in 10% buffer-neutralized formalin solution and embedded in paraffin. Sections were cut at 2 $\mu$m thickness and stained with hematoxylin and eosin.

*Urinalysis and confirmation of the onset of 2DM*

Urine collection was executed by compulsive urination at each weighing time, and urinary glucose was determined by Urolabostick (Biel-Sankyo Co., Ltd., Tokyo). When urinary glucose was detected, blood was collected from the tail vein. Confirmation of the onset of 2DM was decided by the detection of over 300 mg/ml of glucose in blood.

*RT-PCR*

Total RNA was extracted from livers, pancreata, skeletal muscles, and white and brown adipose tissues from 5 mice each of the Meg1 Tg, NOD, KK-A$^y$, BKS, and C57BL/6 strains of mice at 11 weeks of age, using the RNeasy system (QIAGEN K. K., Tokyo) according to the manufacturer's instructions. For the RT-PCR analysis, cDNA was synthesized from 1 $\mu$g of the total RNA using the SuperScript III First-Strand cDNA Synthesis System (Invitrogen Japan K. K., Tokyo) according to the manufacturer's instructions. The cDNA was PCR-amplified in 50 $\mu$l of reaction mixture containing 25 $\mu$l of TaqMan master mix (Applied Biosystems Japan Ltd., Tokyo) and 500 nM of the gene-specific (*Meg1/Grb10*, uncoupling protein 1 (*Ucp1*), glucose transporter 4 (*Glut4*), and *G3PDH* for normalization) TaqManProbe. The assays were performed in triplicate and the copy number of the *Meg1/Grb10*, *Ucp1*, and *Glut4* RNA were

calculated with an ABI Prism 7900 Sequence Detector (Applied Biosystems Japan). The data for each tissue were normalized to an internal standard (*G3PDH*).

*Statistical analysis*

Measurement data are shown as the mean value ± standard error (Mean ± SE). Statistical analysis of the data was performed using a one-factor ANOVA followed by Student's *t*-test. Comparison of the mean was calculated by Bonferroni's method. Covariance analysis was performed by Levene's method. Calculation of confidence limits and significance testing were made at a level of $P$=0.05.

## Results

*Postnatal growth curve*

Fig. 1 shows the body weights of Meg1 Tg mice and controls that were fed either normal fat diet (NFD) or high fat diet (HFD). The weight of Meg1 Tg mice was normal until 4 weeks of age under both NFD and HFD diet conditions. However, their body weights did not increase as much as control mice after weaning and were 12 to 15% smaller than these of control mice at 20 weeks of age. These differences were statistically significant ($P$<0.05).

*Food intake and BMI*

For average food intake, no differences were observed between Meg1 Tg mice and controls under both diet conditions at 11 weeks of age (Fig. 2A: fed with HFD, 1.74 ± 0.02 g/day/10 g of body weight vs 1.65 ± 0.03 g/day/10 g of body weight; and with NFD, 1.65 ± 0.02 g/day/10 g of body weight vs 1.51 ± 0.07 g/day/10 g of body weight). However, BMI of Meg1 Tg mice were significantly lower than these of control mouse fed with HFD ($P$<0.05) both at 15 and 30 weeks of age (Fig. 2B: BMI at 15 weeks of age, 0.27 ± 0.01 g/cm$^2$ vs 0.32 ± 0.03 g/cm$^2$; and at 30 weeks of age, 0.29 ± 0.05 g/cm$^2$ vs 0.36 ± 0.07 g/cm$^2$).

*Glucose tolerance test and insulin tolerance test*

The plasma glucose level of Meg1 Tg mice fed with HFD at 11 weeks of age was significantly higher than those in both Meg1 Tg mice and controls fed with NFD

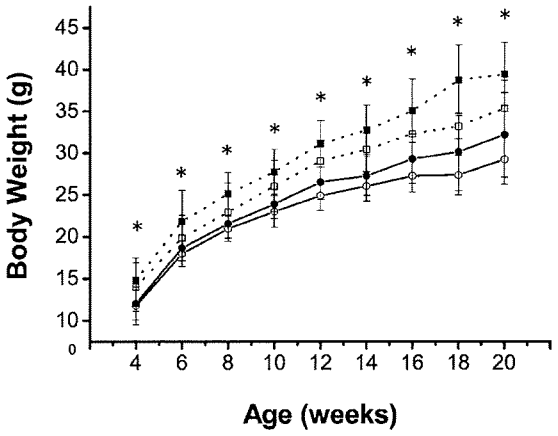


**Fig. 1.** Growth curve of control and Meg1 Tg mice from 4 to 20 weeks of age. Plotted values are means ± SE for 20 mice per group. Open square (□), control mice fed NFD; filled square (■), control mice fed HFD; open circle (○), Meg1 Tg mice fed NFD; filled circle (●), Meg1 Tg mice fed HFD. *$P$<0.05 (Student's *t*-test).

($P$<0.05), indicating that their glucose tolerance was reduced (Fig. 3A). The reduction in blood glucose concentration after intraperitoneal administration of insulin was significantly delayed in Meg1 Tg mice compared to control mice fed with either HFD or NFD ($P$<0.05), indicating that Meg1 Tg mice had insulin resistance (Fig. 3B).

*Organ weight*

The weights of body, visceral fat, and liver, and the visceral fat/body weight ratios and liver/body weight ratios of Meg1 Tg and control mice at 10 to 12 weeks of age are shown in Table 1. The effect on organ weight by HFD feeding in Meg1 Tg mice was examined. When mice were fed HFD, weights of body, visceral fat and livers of Meg1 Tg mice were significantly lower than the controls ($P$<0.05), while liver/body weight ratio of Meg1 Tg mice was significantly higher than that of control mice ($P$<0.05). When Meg1 Tg mice were fed NFD, their body weight was significantly lower than the controls ($P$<0.05). There were no differences in visceral fat/body weight and liver/body weight ratios between Meg1 Tg and control mice irrespective of diet.

*Plasma chemistry*

The data on BUN, TG, insulin, adiponectin, resistin,

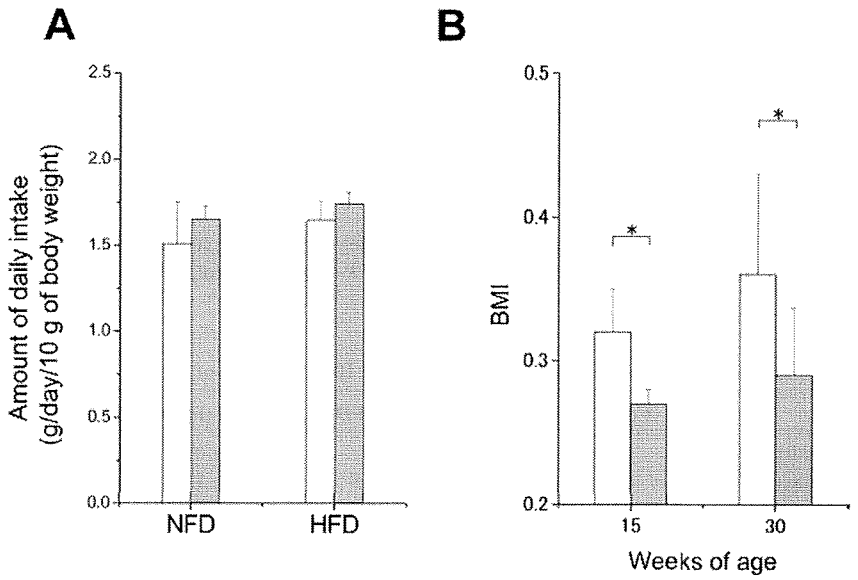


**Fig. 2.** Daily intake and BMI change in control and Meg1 Tg mice. (A) Daily intake of Meg1 Tg (▨) and control (□) mice at 11 weeks of age that were fed with NFD or HFD. There were no significant differences between the diet groups. (B) BMI of Meg1 Tg and control mice fed with HFD were calculated at 15 and 30 weeks of age. BMI of Meg1 Tg mice (▨) at both ages were significantly lower than those of control mice (□) ($P<0.05$).

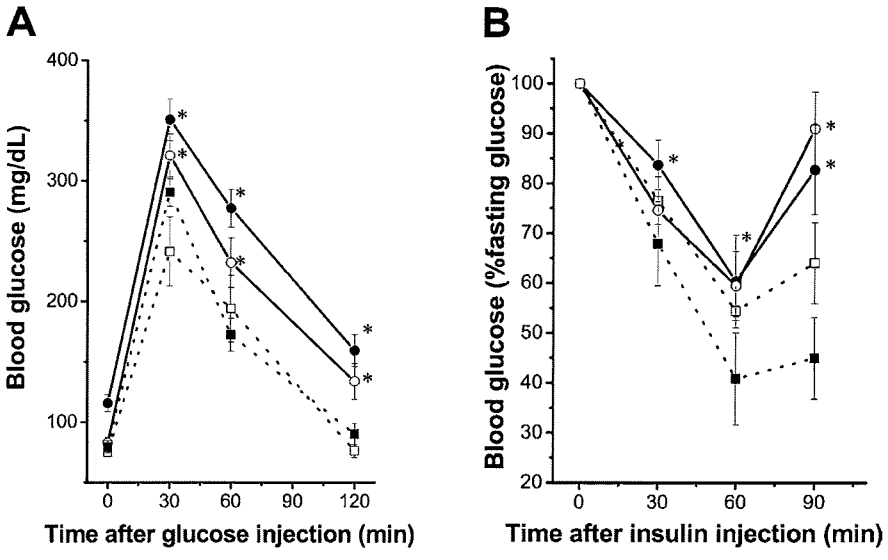


**Fig. 3.** Glucose and insulin tolerance level of Meg1 Tg and control mice. (A) Glucose tolerance in mice at 11 weeks of age that had been fasted overnight (n=10). (B) Insulin tolerance in mice at 11 weeks of age that had been fasted overnight (n=10). Plotted values are means ± SE for 10 mice per group. Open square (□), control mice fed NFD; filled square (■), control mice fed HFD; open circle (○), Meg1 Tg mice fed NFD; filled circle (●), Meg1 Tg mice fed HFD. *$P<0.05$ (Student's $t$-test). Glucose levels and their reduction rate in Meg1 Tg mice were significantly higher than in control mice.

**Table 1.** Liver, fat, and body weights of Meg1Tg and control mice at 10 to 12 weeks of age

| | Control (NFD) | Meg1 Tg (NFD) | Control (HFD) | Meg1 Tg (HFD) |
|---|---|---|---|---|
| Body weight (g) | 20.8 ± 0.6 | 18.4 ± 0.3[a)] | 24.3 ± 0.3 | 19.6 ± 0.4[a)] |
| Visceral fat weight (mg) | 197.6 ± 46.0 | 187.0 ± 68.6 | 507.5 ± 23.0 | 376.7 ± 29.6[a),b)] |
| Visceral fat/body weight ratio (mg/g) | 9.0 ± 0.9 | 8.9 ± 1.6 | 18.8 ± 2.6 | 20.0 ± 1.1 |
| Liver weight (mg) | 900.2 ± 30 | 977.4 ± 38.5 | 1,001.0 ± 15.1 | 906.0 ± 41.8[a)] |
| Liver/body weight ratio (mg/g) | 44.5 ± 3.7 | 51.6 ± 4.9 | 41.2 ± 1.3 | 44.9 ± 2.1[a)] |

Values are the means ± SE for 10 mice per control and 10 mice per Meg1Tg. Meg1Tg (HFD) and control (HFD) mice were fed HFD. Meg1Tg (NFD) and control (NFD) mice were fed NFD. [a)]$P<0.05$ vs control, [b)]$P<0.05$ vs Meg1 Tg (NFD).

**Table 2.** Plasma chemistry in Meg1 Tg and control mice at 10 to 12 weeks of age

| | Control (NFD) | Meg1 Tg (NFD) | Control (HFD) | Meg1 Tg (HFD) |
|---|---|---|---|---|
| BUN (mg/dl) | 26.7 ± 1.9 | 20.6 ± 0.7 | 22.0 ± 0.8 | 19.3 ± 1.2[a)] |
| Triglyceride (mg/dl) | 69.3 ± 23.2 | 90.6 ± 21.9 | 146.3 ± 11.4 | 202.0 ± 23.4[a),b)] |
| Insulin (pg/ml) | 92.5 ± 13.4 | 153.3 ± 14.3 | 88.1 ± 16.9 | 152.4 ± 16.3[a)] |
| Adiponectin (ng/ml) | 23 ± 4.01 | 46.8 ± 3.2 | 48.3 ± 7.0 | 74.4 ± 10.9[a),b)] |
| Resisitin (ng/ml) | 2.28 ± 0.2 | 3.3 ± 0.2 | 3.6 ± 0.2 | 4.0 ± 0.2 |
| IGF-1 (ng/ml) | 395.8 ± 43.1 | 232.5 ± 28.3 | 358 ± 49.5 | 272.1 ± 24.4 |
| Leptin (pg/ml) | 548 ± 171 | 1,136.0 ± 267.0 | 1,036.0 ± 161.0 | 1,008.0 ± 146.0 |
| NH3 ($\mu$g/dl) | 143.1 ± 24.2 | 162.0 ± 12.2 | 223.1 ± 32.6 | 280.7 ± 50.9[b)] |
| Glucose (mg/dl) | 161 ± 16.9 | 163.0 ± 12.6 | 172.8 ± 9.4 | 199.7 ± 58.4 |

Values are the means ± SE for 10 mice per control and 10 mice per Meg1Tg. Meg1Tg (HFD) and control (HFD) mice were fed bHFD. Meg1Tg (NFD) and control (NFD) mice were fed NFD. [a)]$P<0.05$ vs control, [b)]$P<0.05$ vs Meg1Tg(NFD).

IGF-1, leptin, ammonium, and glucose, measured at 10 to 12 weeks of age, are shown in Table 2. Irrespective of diet, plasma BUN in Meg1 Tg mice was significantly lower than in control mice ($P<0.05$). Plasma TG, insulin adiponectin and resistin in Meg1 Tg mice were significantly higher than in control mice ($P<0.05$), whereas plasma IGF-1 of Meg1 Tg mice tended to be lower than in controls. When mice were fed NFD, the plasma leptin concentration of Meg1 Tg mice was significantly higher than that of control mice. For, mice fed HFD, the plasma leptin level of Meg1 Tg mice was almost the same as the value of control mice (Table 2). Plasma glucose and ammonia in both NFD- and HFD-fed Meg1 Tg mice tended to be higher than those of control mice.

Other measured biochemical markers such as TCHO, GOT, GPT, ALP, CPK, and LDH plasma concentrations measured in Meg1 Tg and control mice of the same age were almost similar (data not shown).

*Histological analysis*

We found two histological abnormalities in the pancreatic tissues of Meg1 Tg mice fed NFD: atrophy of the pancreatic acinus cells and an increase in adipocytes at 20 weeks of age; and enlargement of islet of Langerhans (Fig. 4B). When Meg1 Tg mice were fed HFD, the above-noted pathological abnormalities were more severe than these of NFD feeding (Fig. 4C). Pathological abnormalities did not develop in control mice fed NFD or HFD (Fig. 4A).

*The onset rate of type 2 diabetes*

The onset rates of 2DM between Meg1 Tg mouse fed NFD and HFD at 25 weeks were 11.3% and 60.0%, respectively (Fig. 5A). This clearly demonstrates that feeding with HFD induces 2DM in Meg1 Tg mice. There were no symptoms of 2DM in control mice up to 30 weeks of age.

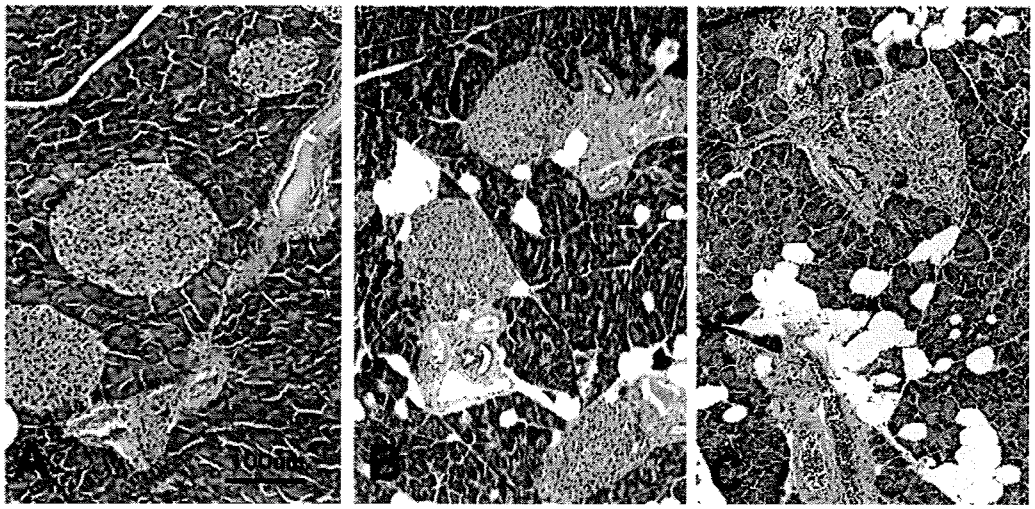

**Fig. 4.** Light microscopic features of pancreata from control and Meg1 Tg mice around 20 weeks of age. Heamatoxylin and eosin stain, × 100. (A) Control mouse. (B) Meg1 Tg mouse fed NFD. (C) Meg1 Tg mouse fed HFD. Vacuolation and denaturation at exocrine pancreas in the Meg1 Tg mouse was found. Furthermore, enlargement of an islet of Langerhans was observed. The pathological abnormality of Meg1 Tg mice fed HFD was more severe than that of NFD-fed Meg1 Tg mice.

### Meg1/Grb10, Ucp1, *and* Glut4 *expression in Meg1 Tg and 3 diabetes model mice*

For further analytical research, we examined diabetes related gene expressions of Meg1 Tg mice in comparison with NOD, KK-A$^y$, BKS, and C57BL/6 mice. *Meg1/Grb10*, *Ucp1*, and *Glut4* expression ratios against control gene are shown in Fig. 6. *Meg1/Grb10* gene expression of skeletal muscle of Meg1 Tg mice was 100 times higher than those of the other 3 diabetes model mice and the C57BL/6 mouse (Fig. 6A: $P<0.05$). In contrast, *Glut4* expression of skeletal muscle of Meg1 Tg mice was significantly lower than these of the 3 diabetes model mice and the C57BL/6 mouse (Fig. 6C: $P<0.05$). There were no differences of *Ucp1* gene expression in brown adipose tissue between Meg1 Tg and the 3 diabetes model mice and the C57BL/6 mouse. Meg1 Tg mice fed HFD showed suppression of *Ucp1* gene expression in brown adipose tissue (Fig. 6).

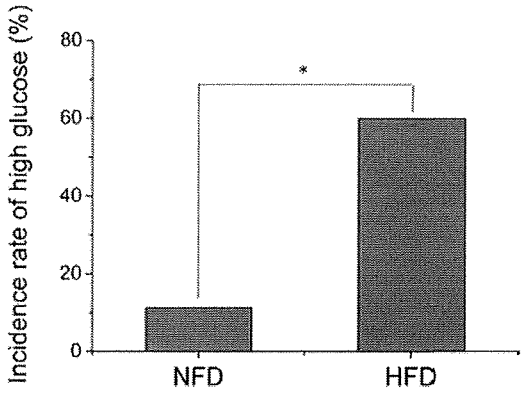


**Fig. 5.** Increased incidence rate of high blood glucose in Meg1 Tg mice fed HDF. Meg1 Tg mice were fed NFD and HFD for 25 weeks. The onset rates (■) of type 2 diabetes, the decided by the detection of over 300 mg/ml of glucose in the blood, in the Meg1 Tg mouse were compared by diet. HFD feeding-induced diabetes was significantly higher than NFD feeding. *$P<0.05$ (Student's $t$-test).

## Discussion

We evaluated the Meg1 Tg mouse as a non-obese 2DM animal model in this study. Two of the major defects seen in 2DM are insulin resistance of targets, such as liver, muscle and adipose tissues, and impaired insulin secretion from pancreatic $\beta$-cells [26, 37, 38]. Histological analysis revealed the pancreatic abnormality in Meg1 Tg mice (Fig. 4). Moreover, Meg1 Tg mice showed both the insulin resistance and glucose intoler-